



Skin barrier lipid enzyme activity in Netherton patients is associated with protease activity and ceramide abnormalities^S

Jeroen van Smeden,^{*,†} Hanin Al-Khakany,^{*} Yichen Wang,[§] Dani Visscher,^{*} Nicole Stephens,^{*} Samira Absalah,^{*} Herman S. Overkleeft,^{**} Johannes M. F. G. Aerts,^{††} Alain Hovnanian,^{§,§§} and Joke A. Bouwstra^{1,*}

Leiden Academic Centre for Drug Research,^{*} Department of Bio-organic Synthesis, Leiden Institute of Chemistry,^{**} and Medical Biochemistry Leiden Institute of Chemistry,^{††} Leiden University, Leiden, The Netherlands; Centre for Human Drug Research,[†] Leiden, The Netherlands; INSERM UMR1163,[§] Imagine Institute, Paris Descartes University, Paris, France; and Department of Genetics,^{§§} Necker-Enfants Malades Hospital, Assistance Publique des Hôpitaux de Paris (AP-HP), Paris, France

ORCID IDs: 0000-0002-2728-2832 (J.v.S.); 0000-0002-7123-6868 (J.A.B.)

Abstract Individuals with Netherton syndrome (NTS) have increased serine protease activity, which strongly impacts the barrier function of the skin epidermis and leads to skin inflammation. Here, we investigated how serine protease activity in NTS correlates with changes in the stratum corneum (SC) ceramides, which are crucial components of the skin barrier. We examined two key enzymes involved in epidermal ceramide biosynthesis, β -glucocerebrosidase (GBA) and acid-sphingomyelinase (ASM). We compared in situ expression levels and activities of GBA and ASM between NTS patients and controls and correlated the expression and activities with *i*) SC ceramide profiles, *ii*) in situ serine protease activity, and *iii*) clinical presentation of patients. Using activity-based probe labeling, we visualized and localized active epidermal GBA, and a newly developed in situ zymography method enabled us to visualize and localize active ASM. Reduction in active GBA in NTS patients coincided with increased ASM activity, particularly in areas with increased serine protease activity. NTS patients with scaly erythroderma exhibited more pronounced anomalies in GBA and ASM activities than patients with ichthyosis linearis circumflexa. They also displayed a stronger increase in SC ceramides processed via ASM. **■** We conclude that changes in the localization of active GBA and ASM correlate with *i*) altered SC ceramide composition in NTS patients, *ii*) local serine protease activity, and *iii*) the clinical manifestation of NTS.—van Smeden, J., H. Al-Khakany, Y. Wang, D. Visscher, N. Stephens, S. Absalah, H. S. Overkleeft, J. M. F. G. Aerts, A. Hovnanian, and J. A. Bouwstra. **Skin barrier lipid enzyme activity in Netherton patients is associated with protease activity and ceramide abnormalities.** *J. Lipid Res.* 2020. 61: 859–869.

Supplementary key words activity-based probe labeling • enzyme expression • ichthyosis linearis circumflexa (Netherton syndrome) • in situ zymography • mass spectrometry • stratum corneum

Netherton syndrome (NTS) is a severe autosomal recessive disorder related to uncontrolled serine protease activity caused by mutations in the serine protease inhibitor Kazal-type 5 (*SPINK5*) gene that encodes for the protease inhibitor, lympho-epithelial Kazal-type-related inhibitor (LEKTI). This protein is crucial for proper skin desquamation (shedding of the skin). Increased epidermal serine protease activity in NTS patients results in scaling and superficial peeling of the skin and skin inflammation (1, 2). Clinical manifestation varies to a high extent: some subjects demonstrate extensive and severe scaly erythroderma, whereas others develop ichthyosis linearis circumflexa (ILC) with variable severity. The origin for this variation is not fully understood (3). Newborns are susceptible to life-threatening dehydration caused by increased water loss resulting from a defective skin barrier function (4). This barrier is primarily located in the stratum corneum (SC) and formed by terminally differentiated keratinocytes (corneocytes) embedded in a lipid matrix (5, 6). This matrix is composed of different lipid classes, like ceramides, cholesterol, and fatty acids. Whereas in other tissues ceramides

Abbreviations: ABP, activity-based probe; ASM, acid sphingomyelinase; GBA, β -glucocerebrosidase; 6-HMU, 6-hexadecanoyl-4-methylumbelliferyl; 6-HMU-PC, 6-hexadecanoyl-4-methylumbelliferyl phosphorylcholine; ILC, ichthyosis linearis circumflexa; NTS, Netherton syndrome; SC, stratum corneum; SG, stratum granulosum.

¹To whom correspondence should be addressed.

e-mail: bouwstra@lacdr.leidenuniv.nl

S The online version of this article (available at <https://www.jlr.org>) contains a supplement.

This work was (financially) supported by the Association Ichtyose France (A.I.F.). The authors declare that they have no conflicts of interest with the contents of this article.

Manuscript received 20 January 2020 and in revised form 31 March 2020.

Published, *JLR Papers in Press*, April 7, 2020

DOI <https://doi.org/10.1194/jlr.RA120000639>

Copyright © 2020 van Smeden et al. Published under exclusive license by The American Society for Biochemistry and Molecular Biology, Inc.

This article is available online at <https://www.jlr.org>

are usually involved in metabolism or cell signaling, ceramides in the SC mainly function as skin barrier components. SC ceramides have very unique features compared with those present in other tissues: *i*) their carbon chains are much longer; and *ii*) there is a large variation in their molecular architecture (subclass overview in supplemental Fig. S1) (7, 8). Ceramides are not synthesized in the SC, but their precursors are synthesized by keratinocytes located in the viable epidermal layers (9, 10). These ceramide precursors (glucosylceramides and sphingomyelins) are subsequently stored in lamellar bodies. These lamellar bodies also contain the enzymes necessary for the final conversion once the lamellar bodies extrude their content into the extracellular environment. This takes place at the interface of the viable epidermis, more specifically the stratum granulosum (SG), and the SC. The extruded ceramide precursors are then converted into their final barrier constituents by one final conversion step: sphingomyelins are converted into ceramides by acid sphingomyelinase (ASM; EC3.1.4.12), whereas glucosylceramides are converted by β -glucocerebrosidase (GBA; EC3.2.1.45). Importantly, GBA may convert glucosyl precursors of all ceramide subclasses, whereas ASM only converts sphingomyelin precursors into subclasses [AS] and [NS] (Fig. 1, supplemental Fig. S1) (11, 12). Thus, conversion by ASM leads to ceramides with a sphingoid base only [see supplemental Fig. S1 for ceramide nomenclature (13)].

Previously, we reported an altered SC ceramide composition in NTS patients (14). However, it is unknown whether this change in ceramide composition is caused by a disbalance of epidermal GBA and ASM enzyme activities in the SC of NTS patients. In addition, the relation between expression/activity of both enzymes and how this relates to the ceramide composition and the clinical manifestation are not understood. Our aim was therefore to localize both expression and activity of ASM and GBA in the epidermis of 10 NTS patients (NTS1–10; denoted as circled numbers 1–10 in the table) and 5 healthy controls. The results provide mechanistic insight into how changes in localization of ASM and GBA associate with increased [AS] and [NS] SC ceramides, and whether this correlates with the localization of protease activity and patient clinical manifestations.

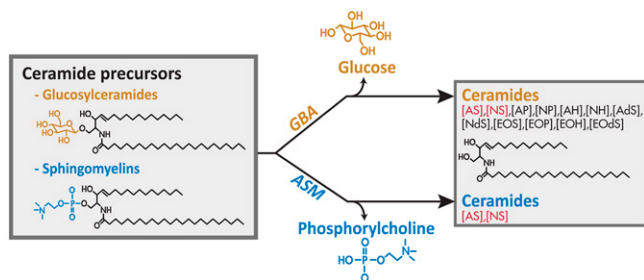


Fig. 1. Schematic overview illustrating the roles of GBA and ASM in human epidermis. Before ceramides become constituents of the SC barrier, a final metabolic conversion takes place in which ceramide precursors, either glucosylceramides or sphingomyelins, are converted by GBA or ASM, respectively.

Subject inclusion and skin processing

The study was conducted according to Declaration of Helsinki principles, with written informed consent from patients (or parents in case of minors). Study approval was obtained from the Comité de Protection des personnes in France (number 101-13). Registration was performed at the French national regulatory agency [Agence Nationale de Sécurité du Médicament (ANSM), number 131066B42]. Ten NTS patients (details in supplemental Table S2 and supplemental Fig. S4) were compared with five healthy controls. SC ceramides were obtained by harvesting SC of the ventral forearm with 10 poly(phenylene sulfide) tape-strips (Nichiban, Tokyo, Japan) prior to ceramide extraction. Four millimeter biopsies were taken for immunohistochemical staining and in situ enzyme activity assays. Concerning NTS patients, all biopsies were from lesional skin sites except for NTS3. Subsequently, biopsies were snap-frozen in liquid nitrogen with matrix specimen (Tissue-Tek O.C.T.; Sakura Finetek Europe, Alphen a/d Rijn, The Netherlands) and cut to 5 μ m-thick sections prior to enzyme studies (see below for more detail and Fig. 2 for an overview of the staining procedures).

Immunohistochemical staining of ASM and GBA

Frozen skin sections were washed in PBS (pH 7.4), blocked with horse serum, and incubated overnight at 4°C with primary antibody for GBA (ab125065; Abcam, Cambridge, UK) and ASM (NBP2-45889; Novus Biologicals, Littleton, CO). Sections were washed in PBS and labeled with secondary antibody for GBA (711-295-152; Jackson ImmunoResearch Laboratories, West Grove, PA) or ASM (ab97035, Abcam). After 1 h incubation period, sections were washed twice in PBS and once in demineralized water and mounted using Vectashield with DAPI (Vector Laboratories, Burlingame, CA).

In situ zymography of active ASM

A new method was developed to visualize active ASM in human skin sections by in situ zymography using 6-hexadecanoyl-4-methylumbelliferylphosphorylcholine (6-HMU-PC) as ASM-specific substrate (Moscerdam, Oegstgeest, The Netherlands). All optimization steps are described in the supplemental Materials and Methods. Briefly, skin sections were washed in 1% (v/v) Tween (Bio-Rad Laboratories, Cambridge, MA). Sections were incubated with 0.5 mM ASM substrate in acetate buffer (pH 5.2) with 0.02% sodium azide and 0.2% sodium taurocholate. Subsequently, samples were washed in 1% Tween solution. Sections were mounted with Vectashield with propidium iodide solution (Vector Laboratories).

In situ activity-based probe labeling of active GBA

Active GBA was visualized using the recently developed activity-based probe (ABP) labeling method (15, 16). Briefly, skin sections were washed for 1 min in 1% (v/v) Tween (Bio-Rad Laboratories) in MilliQ water solution. Subsequently, sections were incubated for 1 h at 37°C with 100 nM ABP MDW941 in McIlvaine buffer [150 mM citric acid- Na_2HPO_4 (pH 5.2), 0.2% (w/v) sodium taurocholate, 0.1% (v/v) Triton X-100]. After incubation, samples were washed once in 1% Tween solution and once in MilliQ water. Sections were mounted with Vectashield with DAPI solution.

In situ zymography of protease activity

Skin sections (5 μ m thickness) of NTS patients embedded in Tissue-Tek O.C.T. compound were dried at room temperature for 10 min and rinsed with 2% Tween 20-PBS solution for 5 min followed by washing two times for 5 min in PBS. Skin sections were incubated overnight at 37°C with 100 μ l of 10 μ g/ml

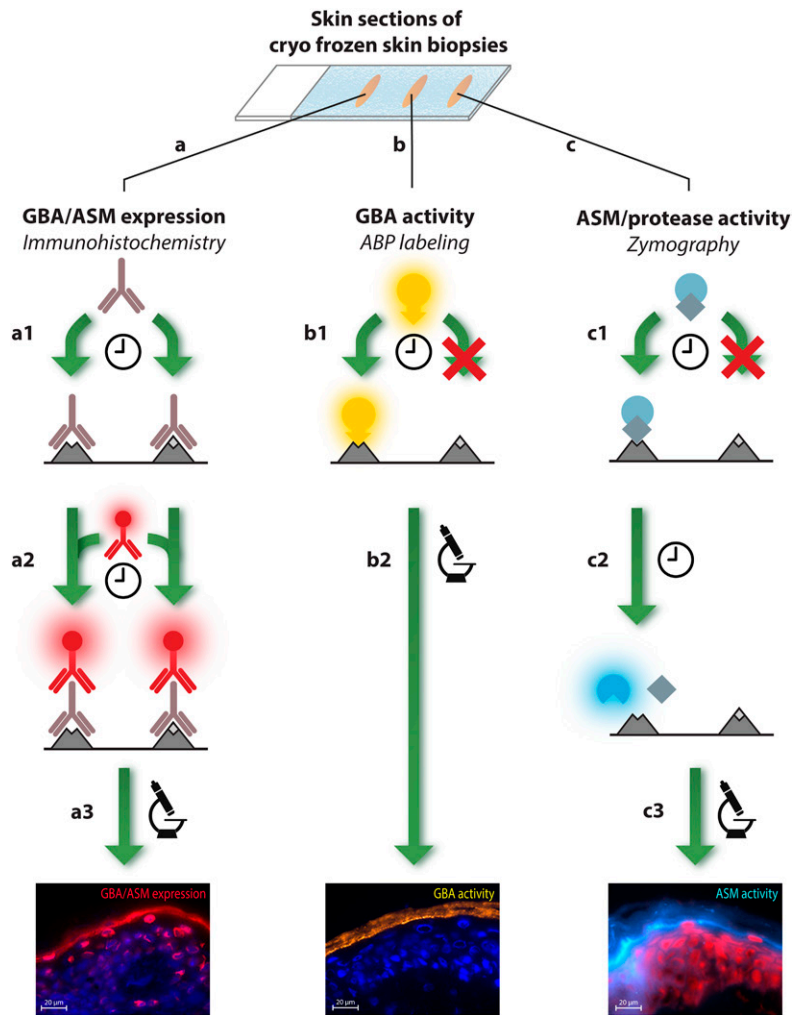


Fig. 2. Overview of all staining methods used to visualize in situ expression and activity of GBA, ASM, and serine protease. Skin sections on microscope glass were treated to one of the different staining procedures: A: Expression of GBA and ASM is achieved via immunohistochemical staining. A1: First, a first antibody (GBA or ASM specific) binds to both active and inactive enzyme during an overnight staining period. A2: After washing procedures, a second antibody with fluorescent label binds to the first antibody in a 1 h incubation period. A3: After a second washing procedure, samples were analyzed by fluorescent microscopy. B: Activity of GBA was visualized by ABP labeling. B1: Skin sections are exposed to a solution of ABP-MDW941, followed by a 1 h incubation period in which the ABP binds with high affinity and specificity to active GBA only. B2: Subsequently, samples are washed, and active GBA is localized via fluorescent microscopy. C: Both protease activity and the new method to visualize ASM activity is established by in situ zymography. C1: First, skin sections are exposed to a solution with substrate that can specifically bind to the enzyme of interest (6-HMU-PC to visualize active ASM, and BODIPY FL casein for serine protease activity). C2: Then, an incubation period is maintained in which the substrate is converted into a product that is fluorescent (1 h for ASM activity, overnight for protease activity). C3: Finally, samples are washed and active ASM or protease is visualized by microscopy. Thus, localization of active enzyme is achieved by visualizing fluorescent product that has been converted by the enzyme of interest. Note that for all methods (A–C), sections were mounted with mounting medium containing a counterstaining solution with DAPI or propidium iodide solution (PI) to stain for nuclei prior to microscope analysis.

BODIPY FL casein (EnzChek Protease Assay Kit; Invitrogen) in 10 mM Tris-HCl buffer (pH 7.8). Subsequently, sections were washed three times with PBS for 5 min and then mounted with Mowiol mounting medium.

Fluorescence microscopy

Protease activity was visualized with a Leica TCS SP8 SMD confocal microscope and analyzed with ImageJ software (<https://imagej.nih.gov/ij/>). All other stainings were imaged using a Zeiss Imager.D2 microscope connected to a Zeiss AxioCam MRm camera (Zeiss, Göttingen, Germany). Images were taken at objective lens magnifications of 20× and 63× (+10× ocular lens magnification). Activity of ASM was visualized by 6-HMU at $\lambda_{\text{ex}} = 380$ nm, $\lambda_{\text{em}} = 460$ nm. Active GBA was visualized with ABP-MDW941 at $\lambda_{\text{ex}} = 549$ nm, $\lambda_{\text{em}} = 610$ nm.

SC ceramide extraction and analysis

A liquid/liquid extraction protocol was used to extract the SC lipids, including the ceramides. This procedure is based on the common methods to extract SC lipids, the Folch extraction, and the Bligh and Dyer extraction (17, 18). Briefly, each SC sample was extracted using three successive extraction steps with different ratios of solvent solutions [chloroform:methanol:water (2:1:0, 1:1:0, 1:2:0.5 v:v:v)]. Afterwards, the fractions of each individual sample were combined and washed with an equal volume of water and 0.25 M KCl to remove possible contaminants from items such as the tape. Subsequently, samples were dried with N_2 gas and the lipids were reconstituted in a solution of

heptane:chloroform:methanol (95:2.5:2.5 v:v:v). Full details on this method (including validation parameters and extraction efficiencies) are described in (19). LC/MS analysis was performed by normal phase chromatography [polyvinyl alcohol (PVA)-silica, 100 × 2.1 mm i.d., 5 μm particle size; YMC, Kyoto, Japan] attached to an Acquity UPLC H-class device (Waters, Milford, MA), programmed with an elution gradient of heptane toward heptane:isopropanol:ethanol (50:25:25). A Xevo TQ-S was used for MS analysis in positive ion mode. LC/MS ceramide data is plotted as relative abundance of internal standard corrected peak areas (percent).

Statistics

For statistics on two independent means, *P*-values were calculated using unpaired *t*-tests with Welch correction (for unequal variances). A two-way ANOVA with a Sidak's multiple comparison test was performed to determine significant differences between the 12 ceramide subclasses for both groups (healthy vs. NTS). Correlations and the corresponding *P*-values are described with the Pearson correlation coefficient.

RESULTS

Abnormal ASM activity and expression in NTS

We developed an in situ zymography method using a selective ASM substrate that results in the fluorogenic product

6-HMU (20). **Figure 3A** demonstrates that, in control skin tissue, active ASM is predominantly localized at the interface between the SG and SC, as well as the innermost SC layers. Fluorescent signal was also observed to a lesser extent in more superficial SC layers and in the viable epidermis. At higher magnifications, individual “striations” of fluorescent signal are observed, illustrating ASM activity in the lipid matrix surrounding the corneocytes. ASM activity is not homogeneously distributed among the striations, indicated by the high regional variance in fluorescence intensity. Figure 3B and C illustrate that ASM is predominantly expressed at the SG/SC interface, and thus resembles to a large extent the results of the ASM activity assay. However, the local variation in intensity that was observed for ASM activity is not observed for the expression, implying that not all expressed ASM is active. In addition, ASM is also de novo expressed in the viable epidermis near the cell nuclei (Fig. 3C).

ASM expression and activity in the epidermis of NTS patients demonstrated large variations between subjects and

even within a single skin section (overview of all individuals in supplemental Fig. S2). NTS patients demonstrate the following differences compared with control skin: *i*) There were areas with intense staining of active ASM near (and also in) parakeratotic cells in the SC (Fig. 3D). *ii*) Other areas showed a reduction or almost complete absence of active ASM at the SG/SC interface compared with control skin. Instead, activity was located in the middle/outermost SC layers and, in some skin sections, showed patchy distribution (Fig. 3E) or was completely absent (supplemental Fig. S2). *iii*) NTS1 and NTS5 demonstrated ASM activity at the SG/SC interface, comparable to control skin (Fig. 3F).

Concerning ASM expression, two types of expression profiles were observed in NTS skin sections: *i*) There were areas that demonstrated high intranuclear expression of ASM, either in parakeratotic cells of the SC (Fig. 3G) and/or throughout upper epidermal cell layers (Fig. 3H). Additionally, extracellular ASM expression in these areas was not focused at the SG/SC interface but primarily manifested as a weak staining throughout (several layers of) the

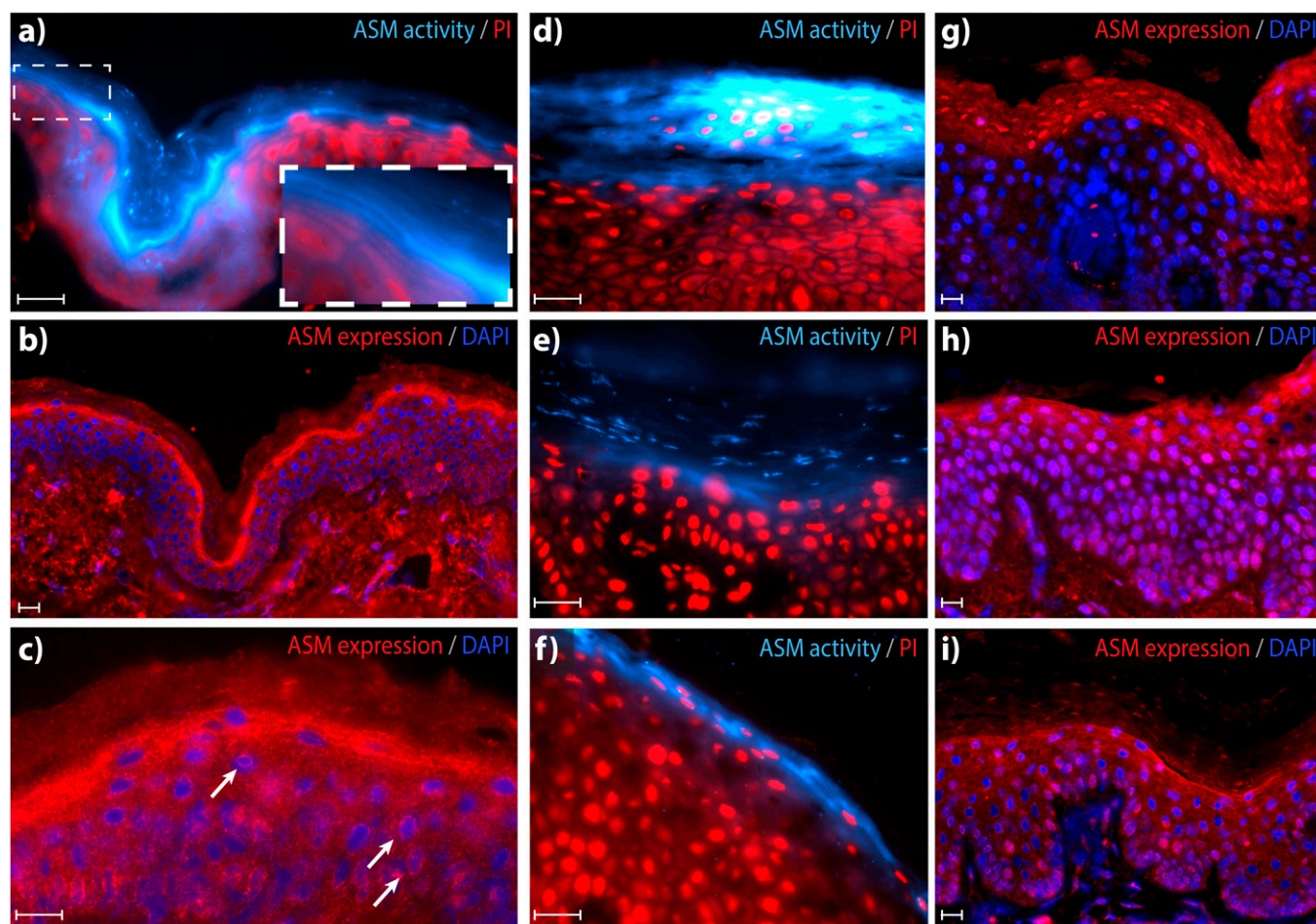


Fig. 3. Epidermal ASM activity and expression in controls (A–C) and NTS (D–I). A: In situ zymography visualizing ASM activity [blue, 63× magnification, counterstaining with propidium iodide solution (PI) (red)]. Inset/zoom illustrates the localization of active ASM in the lipid layers, and the high local variation in active ASM. B: ASM expression [red, 20× magnification, counterstaining with DAPI (blue)]. C: Higher magnification (63×) localizes ASM expression in the SC lipid layers. Arrows indicate location of ASM expressed near nuclei of viable keratinocytes. D–F: Representative in situ zymography of ASM in different NTS patients (63× magnification). G–I: Representative ASM expression in different NTS patients (20× magnification). Note that purple staining indicates nuclei (blue DAPI staining) that also show intense expression of ASM (red). Scale bars represent 20 μ m. See supplemental Fig. S2 for an overview of all individual NTS patients and ASM expression/activity patterns.

epidermis, including the SC. *ii*) There were areas that demonstrated expression at the SG/SC interface; these areas generally showed a diffuse pattern across multiple SC layers (Fig. 3I).

Altered GBA activity and expression in NTS

We compared the GBA activity pattern with the enzyme expression in NTS patients and controls. In control skin, active GBA is not observed in the dermis or viable epidermis, but is evident throughout the entire SC, with increased intensity along the SG/SC interface (Fig. 4A). These striations of fluorescent ABP in the SC illustrate active GBA in the SC lipid matrix layers. Staining was not homogeneously distributed, indicating that active GBA is not equally present throughout the SC.

This profile changed drastically in NTS subjects, and a large variance within and between patients was observed. In general, GBA activity was either significantly lower (sometimes hardly present at all, Fig. 4B) or demonstrated a more diffuse pattern with low signal of active GBA located throughout all epidermal layers (Fig. 4C). NTS skin sections with no visible parakeratosis and a generally more normal appearing morphology showed GBA activity either at the SG/SC interface or throughout all SC layers (Fig. 4D).

Regarding GBA expression, control skin showed a concentrated band at the SG/SC interface and lower SC layers, and there was less expression in upper SC layers (Fig. 4E). De novo-synthesized GBA enzyme was also visible surrounding the nuclei of some epidermal cells, particularly those close to the SG/SC interface. In skin sections of NTS patients, GBA-expression was highly variable between and within subjects: Five NTS subjects demonstrated some skin section areas in which GBA expression was comparable to controls, showing a clear expression at the SG/SC interface (Fig. 4F). For the other skin areas and the other five NTS subjects, GBA expression appeared (partially) in the intracellular space throughout the viable epidermis, either with or without a more intense expression at the SG and SC transition area (Fig. 4G). This expression pattern was particularly seen at skin areas with substantial parakeratosis.

Inverse correlation between GBA activity and ASM activity in single NTS skin sections

When analyzing complete skin sections from each NTS patient, six out of ten patients demonstrate a varying expression and/or activity profile along each section (multiple skin sections per subject were analyzed). **Figure 5** demonstrates a representative example of these six patients for whom the following correlations were observed: *i*) In areas with substantial active GBA, almost no active ASM was observed (Fig. 5A–D, compare area 1 with area 3). These areas had a relatively normal morphology with GBA-expression comparable to control skin. *ii*) Skin section areas with an abnormal morphology (particularly near parakeratotic cells) showed a drastic increase of active ASM, sometimes also within the corneocytes instead of being localized in the lipid matrix (Fig. 5A–D, compare area 2 with area 4). *iii*) Areas with a mediocre intensity staining of active ASM

(e.g., not absent, not intense/focused) also demonstrated mediocre intensities of active GBA (for example, NTS3 and NTS4 in supplemental Fig. S2). In general, there was strong evidence for an inverse relationship between the activity of GBA and ASM, rather than with the expression of both enzymes.

Localization of active GBA and ASM coincide with serine protease activity

Next, we compared the localization of the lipid enzymes with the localization of serine protease activity, generally not abundantly present in control skin (supplemental Fig. S2). In contrast, NTS subjects had a large variation in serine protease activity, as observed for the activity of ASM and GBA. For individual subjects, areas with increased serine protease activity matched areas with enhanced ASM activity and decreased/absent GBA activity. This is illustrated for NTS7 in Fig. 5.

Altered SC ceramide composition in NTS

Metabolic processes of GBA and ASM directly affect the SC ceramide composition. **Figure 6A** shows the ceramide profile (expressed as relative peak areas) of the 12 most prominent ceramide subclasses from SC of controls versus NTS patients (individual data in supplemental Fig. S3). SC ceramide data of NTS7 was excluded due to an extremely low amount of detected lipid content, leading to data that could be easily misinterpreted. In general, controls had a comparable ceramide composition with ceramide [NP] the most abundant (21, 22). NTS patients demonstrated a strong reduction in ceramide [NP] and a significant increase in sphingosine ceramides [NS] and [AS], the only two ceramide subclasses that are enzymatic products of sphingomyelin by ASM (11, 12). **Figure 6B** shows that the abundance of these subclasses varied enormously among NTS subjects. Abundances of ceramides [AS] and [NS] strongly correlated ($R^2 = 0.94$, Fig. 6C). In addition, the fraction of very long [EO] ceramides generally decreased in NTS patients (Fig. 6D). These [EO] ceramides can only be synthesized via GBA and are crucial for a proper skin barrier.

NTS clinical presentation aligns with SC ceramide abnormalities and their respective processing enzyme activity

Table 1 provides an overview of the analyzed parameters and the clinical characteristics for each individual NTS patient. The supplement contains specific information on the scoring procedure for each individual. It became apparent that GBA and/or ASM expression did not correlate with the clinical form defined as scaly erythroderma or ILC. However, (except for NTS2) proteolytic activity tended to be more elevated in NTS patients with scaly erythroderma than in patients with ILC. Proteolytic activity was increased at areas with increased ASM activity and decreased GBA activity. Moreover, a relation between the clinical form and the activity score of GBA and ASM was observed. Additionally, the increase in the abundance of SC ceramides [AS] and [NS] and the reduction in [EO] ceramide amounts were more pronounced in patients with scaly erythroderma

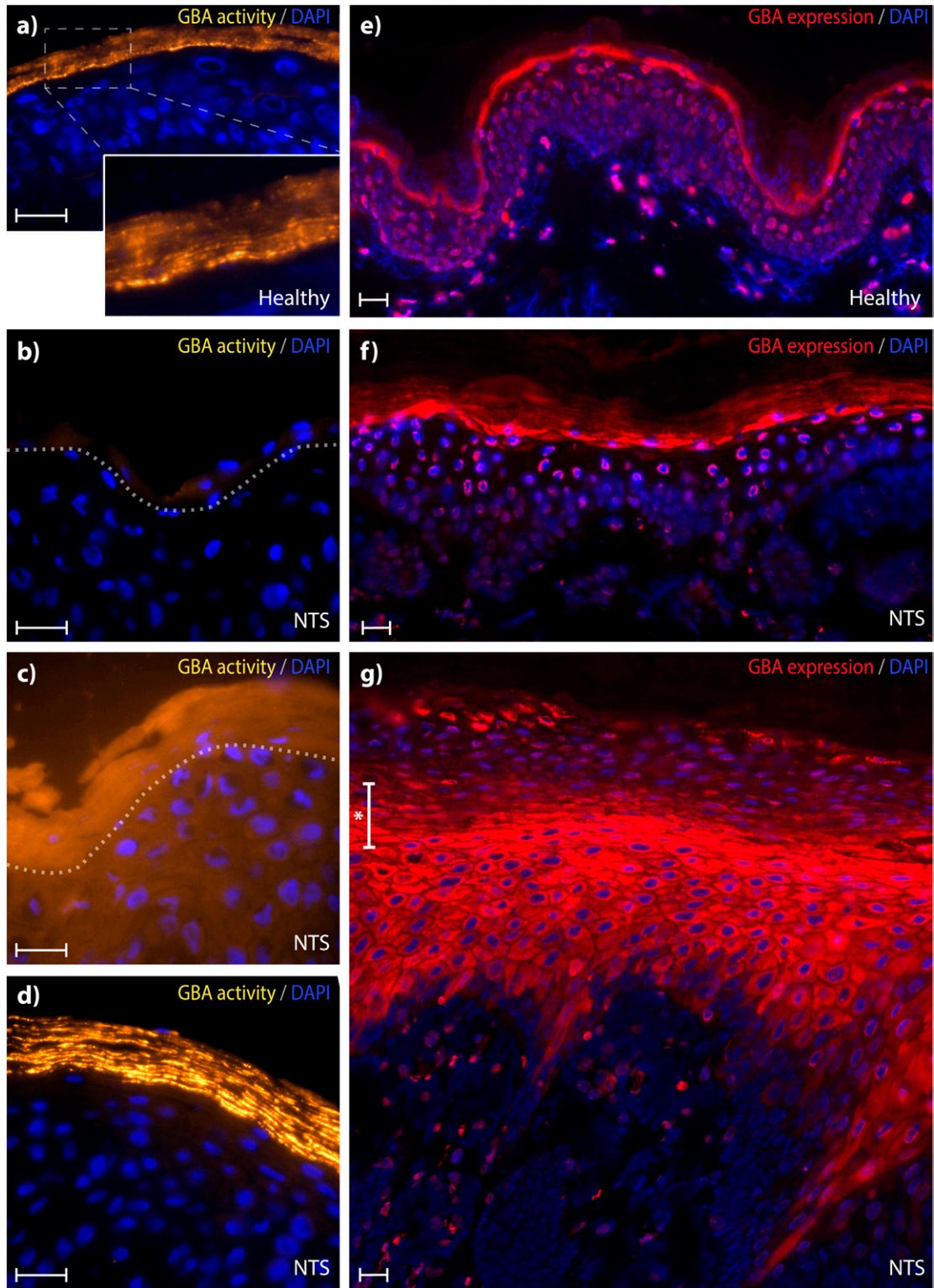


Fig. 4. GBA staining in controls and NTS skin sections. a–d: Active GBA (yellowish, 63× magnification). A: GBA labeling representative for control subjects including a magnified area demonstrating labeling in the SC lipid layers. B–D: Three representative images for three different GBA activity patterns observed in NTS subjects. Dotted gray lines represent the SG/SC interface. E–G: Skin sections stained for expressed GBA (red, 20× magnification) of control human skin (E) and two types of expression profiles representative for all NTS subjects (F, G). At areas with parakeratosis, usually a narrow staining at the SG/SC interface was not present; rather, a transition area was observed (indicated by *). In all sections, DAPI (blue) was used as counterstaining. Scale bar represents 20 μm . See supplemental Fig. S2 for an overview of all individual NTS patients and GBA expression/activity patterns.

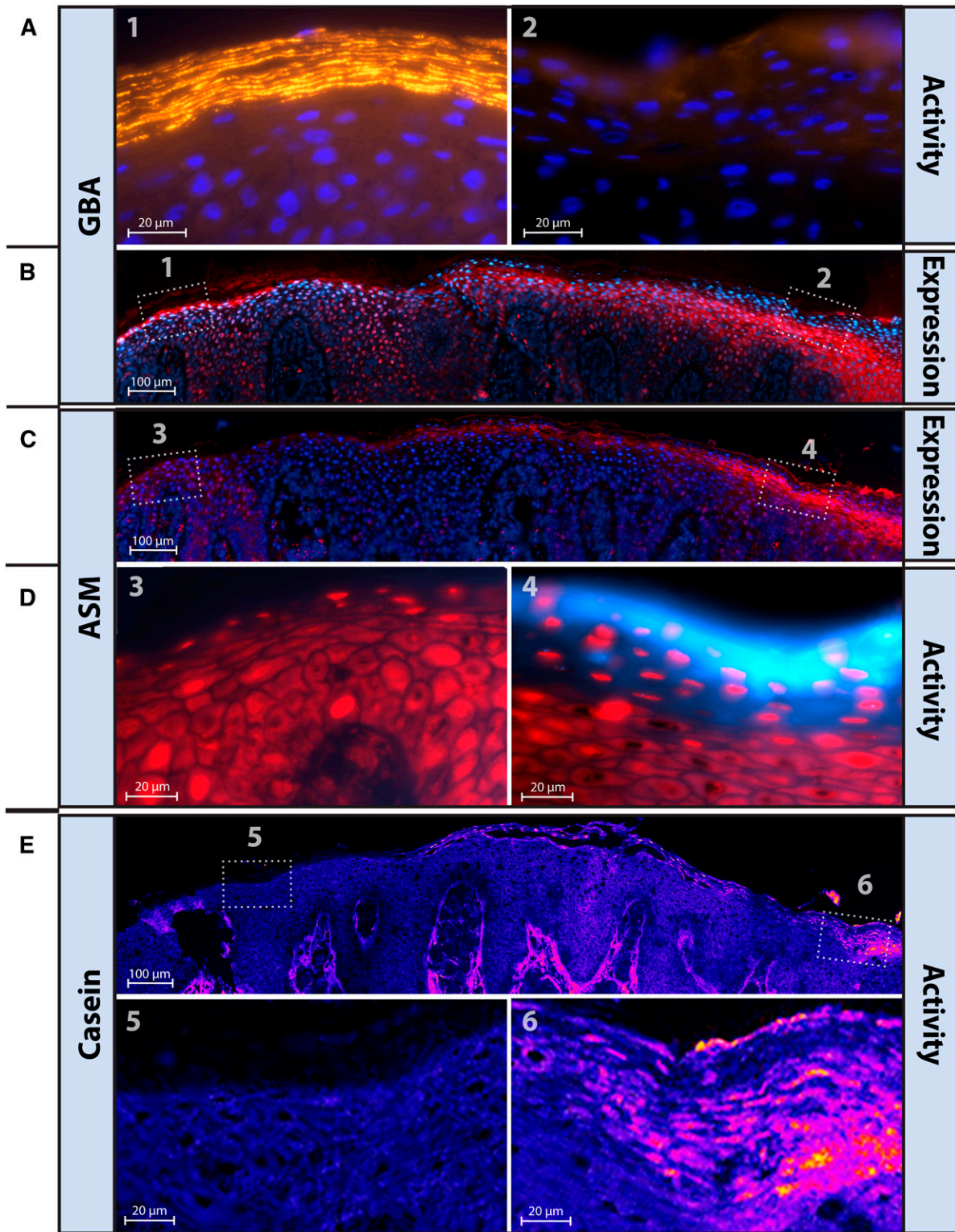


Fig. 5. High local variation in GBA, ASM, and protease staining and/or activity in NTS patients. Five different stainings on five sequential 5 μ m cut cryo-frozen sections from NTS7 and presented with matching skin areas. A: GBA-activity (yellowish, 63 \times magnification) from two different areas (areas 1 and 2) within a single cut section (blue, DAPI counterstaining). B, C: Respectively, GBA and ASM expression, labeled in red (with DAPI as blue counterstaining, magnification 20 \times). D: ASM activity (light blue, 63 \times magnification) from two different areas (areas 3 and 4) within a single cut section (red, propidium iodide solution (PI) counterstaining). E: Serine protease activity is shown in purple/orange (63 \times magnification) including a magnified area illustrating active serine proteases at some areas in the SC lipid layers.

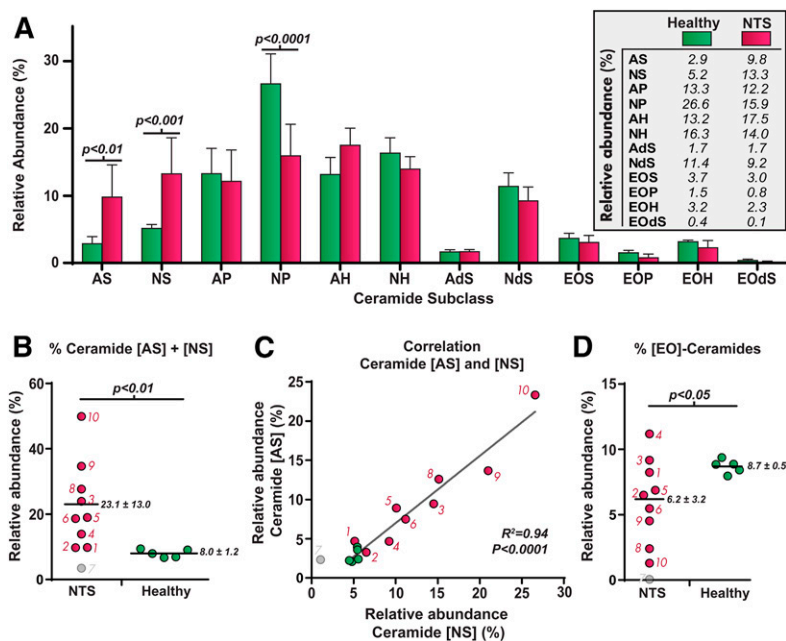


Fig. 6. Data on the SC ceramides in controls (green) and NTS-patients (red). **A:** Bar plot of the ceramide abundances (presented as relative peak area percent) of the 12 ceramide subclasses (mean \pm 95% CI). *P*-values were calculated using a two-way ANOVA with Sidak's multiple comparison test. **B, C:** Dot plot and correlation plot of ceramides [AS] + [NS]. As explained in the text, NTS7 was excluded in all statistical analyses (including NTS7 changes R^2 value to 0.93). **D:** Dot plots of the [EO] ceramides, known to be important for a proper skin barrier function. Horizontal lines and their corresponding values indicate mean \pm SD. Unpaired *t*-tests with Welch correction were used to obtain *P*-values for B and D.

compared with patients with ILC and were not observed in patients with minor forms of ILC.

DISCUSSION

This study is the first to assess and localize the expression and activity of both GBA and ASM in NTS. The new zymography method that we applied uses 6-HMU-PC. This is, according to literature, a more robust and selective substrate alternative than the standard Amplex red peroxidase/choline oxidase assay (20, 23). The developed method is also less labor intensive and enabled us to visualize with high spatial resolution active ASM in human epidermis. Together with GBA activity labeling, we could localize both active enzymes in the SC lipid layers of NTS patients and controls. This allowed us to relate activity of key lipid-processing enzymes GBA and ASM to the ceramide profile.

GBA activity is abnormal in NTS

NTS patients demonstrated abnormal GBA expression and activity, particularly at areas with parakeratosis. GBA was still expressed in most NTS patients, but only minimally active at the SC/SG interface where lipid synthesis and metabolism are crucial for optimal formation of the lamellar layers (24). A change in the local cellular environment (e.g., local pH, discussed below) or the absence of activator protein saposin-C (25, 26) may be underlying factors. Reduced/inactive GBA will lead to a cell-mediated response in which GBA expression is upregulated by the cell to maintain homeostasis (27), explaining GBA overexpression in several NTS subjects.

Increased ASM activity correlates with the abundance of ceramides [AS] and [NS]

The increase in ASM activity can (at least in part) explain the increment in subclasses [AS] and [NS] in NTS, as those ceramides are reported to be the only subclasses that

originate from conversion of sphingomyelins by ASM (besides by GBA) (11, 12). The strong correlation between ceramides [NS] and [AS] (and between no other ceramides; supplemental Table S1) supports this relationship. It is known that ceramides [AS] and particularly [NS] function as second-messenger molecules in case of cellular stress or an inflammatory response (28–30). ASM is a key mediator, upregulated under these circumstances, leading to increased activity in parakeratotic cells. This induces an increase in [AS] and [NS] ceramides (31, 32) and ultimately an increase in sphingosine-1-phosphate, a strong immunoregulator for trafficking of T- and B-cells (33–35). Both altered expression of ASM and elevated levels of ceramides [AS] and [NS] are also related to skin diseases like atopic dermatitis and psoriasis (13, 36–38). It is reported that SC from these diseases shows a decrease in ceramide [NP], similar to what is observed in our NTS cohort. These changes in the SC ceramide composition observed in NTS and other inflammatory skin diseases indicate that the activity of GBA and ASM may also be altered in other diseases. The fact that patients with scaly erythroderma (NTS8, NTS9, and NTS10) also demonstrate highly active ASM in parakeratotic cells supports the role of ASM as a mediator of stress/inflammation (39). This is in line with the observations of altered lamellar body secretion in NTS patients and granules in SC areas with parakeratotic cells (40–42). In our NTS cohort, the extent of parakeratosis related with the location and intensity of active ASM: *i*) SC areas without parakeratosis had either very limited activity or active ASM confined to the SC/SG interface (comparable to control skin). *ii*) Conversely, areas of very thick heavily nucleated SC, as seen in NTS2, NTS6, NTS7, and NTS9, had intense ASM activity staining.

Protease activity matches GBA and ASM activity

Another key finding from this study is the mutual relationship between GBA, ASM, and serine protease activities.

TABLE 1. Overview of the individual NTS-subjects and their resemblance to control skin

Subject	Clinical form	GBA+ASM enzymes		SC Ceramides		Protease
		Expression Score	Activity Score	[AS]+[NS] (%)	[EO] (%)	Activity Score
NTS1	Minor ILC	++	+	9.8	8.2	+
NTS2	Minor ILC	+++	++	9.8	6.5	+++
NTS3	Extensive ILC	○	++	24.0	9.2	○
NTS4	Extensive ILC	○	++	13.9	11.2	○
NTS5	Extensive ILC	+++	+	19.0	6.9	+
NTS6	Extensive ILC	+	++	18.7	5.5	+
NTS7	Extensive ILC	++	++	3.5*	0.0*	++
NTS8	Scaly erythroderma	++	+++	27.7	2.4	+++
NTS9	Scaly erythroderma	+++	+++	34.7	4.5	+++
NTS10	Scaly erythroderma	++	+++	50.0	1.3	ND
Control	Healthy (n=5)	○	○	8.0 ± 1.2	8.7 ± 0.5	○

Each NTS-subject (denoted NTS1 to NTS10) was characterized for the clinical form, and scored on enzymes GBA+ASM, the ceramide composition, and the protease activity. Scoring for expression and activity of lipid enzymes and protease was performed by classifying them among 4 subgroups: resembling control skin (○), mild changes (+), medium changes (++), or very different compared with control skin (+++). Values of the SC ceramides are the relative abundance of the respective subclasses (± SD for the healthy control group). ND indicates, not determined, * indicates unreliable outcomes (see text).

Although NTS patients demonstrated an extensive variation in the localization of active enzyme, a decrease in GBA activity coincided with an increase in both ASM activity and serine protease activity. Particularly for NTS2, NTS6, NTS7, and NTS9, this colocalization is most apparent at heavily nucleated SC areas (supplemental Fig. S2). In contrast, the absence of serine protease activity correlated with the presence of active GBA. This implies a direct or indirect link between epidermal proteases and these lipid enzymes. One such common factor could be the local skin pH. The acidic environment of the SC (between pH 4 and 6) is crucial for epidermal barrier integrity, lipid enzyme function, and serine protease activity (43). Changes in skin pH directly affect enzyme activity of lipid enzymes like GBA and ASM, which may lead to incompletely processed lamellar membranes and a disruptive skin barrier (23). Moreover, an increase in local skin pH in NTS will lead to further increased protease activity of kallikreins 5 and 7 (besides the increment due to LEKTI deficiency). These proteases are involved in the desquamation process and degradation of lipid processing enzymes like GBA and ASM (23, 44). Indeed, NTS patients suffer from defective Kallikrein 5/7 inhibition, which may contribute to the defective skin barrier in these patients (42, 45). The increase in ceramides [AS] and [NS] will contribute to a more permeable barrier, as demonstrated with lipid membranes in which these ceramide subclasses were increased (46).

Correlation with clinical form of NTS

Finally, we elaborate on the relation between the clinical manifestations of the 10 NTS subjects and the relation with SC lipids and lipid enzymes. No clear correlation between the expression of GBA/ASM and the clinical form was observed, in line with our previous study in NTS (14): NTS3 and NTS4 had extensive ILC, but their expression closely resembled that of healthy skin. Additionally, NTS1 and NTS2 were diagnosed with a minor form


of NTS but did show major differences in both GBA and ASM expression.

Strikingly, activity scores of both enzymes matched the clinical form of almost all subjects very well: all subjects demonstrated deviations in ASM+GBA activity compared with control skin, including mild forms of NTS or nonlesional skin (NTS3), and also displayed altered ASM+GBA activity. Marked abnormal localization of GBA+ASM activity was associated with the most severe form of NTS with scaly erythroderma (NTS8, NTS9, and NTS10). These subjects also demonstrated the highest levels of [AS] and [NS] ceramides. In contrast, NTS1 and NTS2, who had a minor form of NTS, displayed a ceramide composition that was (of all NTS subjects) most comparable to control skin.

Future research on NTS patients as well as other patients with skin diseases that demonstrate similar changes in SC lipids (e.g., psoriasis, atopic dermatitis) could elucidate whether the observed changes in SC ceramide subclasses and their respective enzyme profile (expression and activity) is a unique feature of NTS or a more general profile for skin diseases. The toolbox of methods combined in this NTS study may be used for a better understanding of the disease and may even assist in diagnosing (the severity of) NTS in individual patients. Current diagnosis of NTS focuses on dermatological findings or by trichoscopy (hair and scalp structure evaluation), which may sometimes prove difficult or could, even today, lead to missed cases, in which misdiagnosis occurred for many years (47). Current DNA screening tests for SPINK5 mutations are, in practice, not feasible for daily diagnostic confirmation. Therefore, analysis of the ceramides and the respective enzyme expression/activity localization can be useful as a complementary method that may assist in diagnosing these patients.

Overall, the introduction of a new method to analyze both expressed and active ASM and GBA in situ enabled us to reveal the relation between these lipid enzymes, the protease activity, and the SC ceramide composition in NTS patients. In addition, we demonstrate that differences in these enzyme activities relate to the clinical form of NTS.

Data availability

Original datasets related to this article can be found at Mendeley Data (<http://dx.doi.org/10.17632/wr9nw7vhm9.1>), (van Smeden, 2019). All other data are included in the article. 

The authors thank Jannik Rousel and Walter Boiten for assisting in quantifying LC/MS data and Mathilde Bonnet des Claustres for technical assistance. The authors are grateful to the Association Ichtyose France (A.I.F.) for their (financial) support.

REFERENCES

- Greene, S. L., and S. A. Muller. 1985. Netherton's syndrome. Report of a case and review of the literature. *J. Am. Acad. Dermatol.* **13**: 329–337.
- Traupe, H. 1989. *The Ichthyoses: A Guide to Clinical Diagnosis, Genetic Counseling, and Therapy.* Springer-Verlag, Berlin, New York.

3. Bitoun, E., S. Chavanas, A. D. Irvine, L. Lonie, C. Bodemer, M. Paradisi, D. Hamel-Teillac, S. Ansai, Y. Mitsuhashi, A. Taieb, et al. 2002. Netherton syndrome: disease expression and spectrum of SPINK5 mutations in 21 families. *J. Invest. Dermatol.* **118**: 352–361.
4. Stoll, C., Y. Alembik, D. Tchomakov, J. Messer, E. Heid, N. Boehm, P. Calvas, and A. Hovnanian. 2001. Severe hypernatremic dehydration in an infant with Netherton syndrome. *Genet. Couns.* **12**: 237–243.
5. Elias, P. M., and G. K. Menon. 1991. Structural and lipid biochemical correlates of the epidermal permeability barrier. *Adv. Lipid Res.* **24**: 1–26.
6. Proksch, E., R. Folster-Holst, and J. M. Jensen. 2006. Skin barrier function, epidermal proliferation and differentiation in eczema. *J. Dermatol. Sci.* **43**: 159–169.
7. van Smeden, J., and J. A. Bouwstra. 2016. Stratum corneum lipids: their role for the skin barrier function in healthy subjects and atopic dermatitis patients. *Curr. Probl. Dermatol.* **49**: 8–26.
8. Masukawa, Y., H. Tsujimura, and H. Narita. 2006. Liquid chromatography-mass spectrometry for comprehensive profiling of ceramide molecules in human hair. *J. Lipid Res.* **47**: 1559–1571.
9. Holleran, W. M., Y. Takagi, G. K. Menon, G. Legler, K. R. Feingold, and P. M. Elias. 1993. Processing of epidermal glucosylceramides is required for optimal mammalian cutaneous permeability barrier function. *J. Clin. Invest.* **91**: 1656–1664.
10. Schmuth, M., M. Q. Man, F. Weber, W. Gao, K. R. Feingold, P. Fritsch, P. M. Elias, and W. M. Holleran. 2000. Permeability barrier disorder in Niemann-Pick disease: sphingomyelin-ceramide processing required for normal barrier homeostasis. *J. Invest. Dermatol.* **115**: 459–466.
11. Hamanaka, S., M. Hara, H. Nishio, F. Otsuka, A. Suzuki, and Y. Uchida. 2002. Human epidermal glucosylceramides are major precursors of stratum corneum ceramides. *J. Invest. Dermatol.* **119**: 416–423.
12. Uchida, Y., M. Hara, H. Nishio, E. Sidransky, S. Inoue, F. Otsuka, A. Suzuki, P. M. Elias, W. M. Holleran, and S. Hamanaka. 2000. Epidermal sphingomyelins are precursors for selected stratum corneum ceramides. *J. Lipid Res.* **41**: 2071–2082.
13. Motta, S., M. Monti, S. Sesana, R. Caputo, S. Carelli, and R. Ghidoni. 1993. Ceramide composition of the psoriatic scale. *Biochim. Biophys. Acta.* **1182**: 147–151.
14. van Smeden, J., M. Janssens, W. A. Boiten, V. van Drongelen, L. Furio, R. J. Vreeken, A. Hovnanian, and J. A. Bouwstra. 2014. Intercellular skin barrier lipid composition and organization in Netherton syndrome patients. *J. Invest. Dermatol.* **134**: 1238–1245.
15. van Smeden, J., I. M. Dijkhoff, R. W. J. Helder, H. Al-Khakany, D. E. C. Boer, A. Schreuder, W. W. Kallemeijn, S. Absalah, H. S. Overkleeft, J. Aerts, et al. 2017. In situ visualization of glucocerebrosidase in human skin tissue: zymography versus activity-based probe labeling. *J. Lipid Res.* **58**: 2299–2309.
16. Witte, M. D., W. W. Kallemeijn, J. Aten, K. Y. Li, A. Strijland, W. E. Donker-Koopman, A. M. van den Nieuwendijk, B. Bleijlevens, G. Kramer, B. I. Florea, et al. 2010. Ultrasensitive in situ visualization of active glucocerebrosidase molecules. *Nat. Chem. Biol.* **6**: 907–913.
17. Folch, J., M. Lees, and G. H. Sloane Stanley. 1957. A simple method for the isolation and purification of total lipides from animal tissues. *J. Biol. Chem.* **226**: 497–509.
18. Bligh, E. G., and W. J. Dyer. 1959. A rapid method of total lipid extraction and purification. *Can. J. Biochem. Physiol.* **37**: 911–917.
19. Boiten, W., S. Absalah, R. Vreeken, J. Bouwstra, and J. van Smeden. 2016. Quantitative analysis of ceramides using a novel lipidomics approach with three dimensional response modelling. *Biochim. Biophys. Acta.* **1861**: 1652–1661.
20. van Diggelen, O. P., Y. V. Voznyi, J. L. Keulemans, K. Schoonderwoerd, J. Ledvinova, E. Mengel, M. Zschiesche, R. Santer, and K. Harzer. 2005. A new fluorimetric enzyme assay for the diagnosis of Niemann-Pick A/B, with specificity of natural sphingomyelinase substrate. *J. Inherit. Metab. Dis.* **28**: 733–741.
21. van Smeden, J., M. Janssens, G. S. Gooris, and J. A. Bouwstra. 2014. The important role of stratum corneum lipids for the cutaneous barrier function. *Biochim. Biophys. Acta.* **1841**: 295–313.
22. Masukawa, Y., H. Narita, H. Sato, A. Naoe, N. Kondo, Y. Sugai, T. Oba, R. Homma, J. Ishikawa, Y. Takagi, et al. 2009. Comprehensive quantification of ceramide species in human stratum corneum. *J. Lipid Res.* **50**: 1708–1719.
23. Hachem, J. P., M. Q. Man, D. Crumrine, Y. Uchida, B. E. Brown, V. Rogiers, D. Roseeuw, K. R. Feingold, and P. M. Elias. 2005. Sustained serine proteases activity by prolonged increase in pH leads to degradation of lipid processing enzymes and profound alterations of barrier function and stratum corneum integrity. *J. Invest. Dermatol.* **125**: 510–520.
24. Fartasch, M. 2004. The epidermal lamellar body: a fascinating secretory organelle. *J. Invest. Dermatol.* **122**: XI–XII.
25. Atrian, S., E. Lopez-Vinas, P. Gomez-Puertas, A. Chabas, L. Vilageliu, and D. Grinberg. 2008. An evolutionary and structure-based docking model for glucocerebrosidase-saposin C and glucocerebrosidase-substrate interactions - relevance for Gaucher disease. *Proteins.* **70**: 882–891.
26. Ben Bdira, F., W. W. Kallemeijn, S. V. Oussoren, S. Scheij, B. Bleijlevens, B. I. Florea, C. van Roomen, R. Ottenhoff, M. van Kooten, M. T. C. Walvoort, et al. 2017. Stabilization of glucocerebrosidase by active site occupancy. *ACS Chem. Biol.* **12**: 1830–1841.
27. Lu, J., J. Chiang, R. R. Iyer, E. Thompson, C. R. Kaneski, D. S. Xu, C. Yang, M. Chen, R. J. Hodes, R. R. Lonsler, et al. 2010. Decreased glucocerebrosidase activity in Gaucher disease parallels quantitative enzyme loss due to abnormal interaction with TCP1 and c-Cbl. *Proc. Natl. Acad. Sci. USA.* **107**: 21665–21670.
28. Peña, L. A., Z. Fuks, and R. Kolesnick. 1997. Stress-induced apoptosis and the sphingomyelin pathway. *Biochem. Pharmacol.* **53**: 615–621.
29. Hannun, Y. A. 1996. Functions of ceramide in coordinating cellular responses to stress. *Science.* **274**: 1855–1859.
30. Reed, J. C., and D. R. Green. 2011. Apoptosis: Physiology and Pathology. Cambridge University Press, Cambridge, UK.
31. Jenkins, R. W., D. Canals, and Y. A. Hannun. 2009. Roles and regulation of secretory and lysosomal acid sphingomyelinase. *Cell. Signal.* **21**: 836–846.
32. Zheng, W., J. Kollmeyer, H. Symolon, A. Momin, E. Munter, E. Wang, S. Kelly, J. C. Allegood, Y. Liu, Q. Peng, et al. 2006. Ceramides and other bioactive sphingolipid backbones in health and disease: lipidomic analysis, metabolism and roles in membrane structure, dynamics, signaling and autophagy. *Biochim. Biophys. Acta.* **1758**: 1864–1884.
33. Ohkawa, R., M. Kurano, Y. Mishima, T. Nojiri, Y. Tokuhara, T. Kishimoto, K. Nakamura, S. Okubo, S. Hosogaya, Y. Ozaki, et al. 2015. Possible involvement of sphingomyelin in the regulation of the plasma sphingosine 1-phosphate level in human subjects. *Clin. Biochem.* **48**: 690–697.
34. Herzinger, T., B. Kleuser, M. Schafer-Korting, and H. C. Korting. 2007. Sphingosine-1-phosphate signaling and the skin. *Am. J. Clin. Dermatol.* **8**: 329–336.
35. Alessenko, A. V. 2000. The role of sphingomyelin cycle metabolites in transduction of signals of cell proliferation, differentiation and death. *Membr. Cell Biol.* **13**: 303–320.
36. Jensen, J. M., R. Folster-Holst, A. Baranowsky, M. Schunck, S. Winoto-Morbach, C. Neumann, S. Schutze, and E. Proksch. 2004. Impaired sphingomyelinase activity and epidermal differentiation in atopic dermatitis. *J. Invest. Dermatol.* **122**: 1423–1431.
37. Japtok, L., W. Baumer, and B. Kleuser. 2014. Sphingosine-1-phosphate as signaling molecule in the skin: Relevance in atopic dermatitis. *Allergo J. Int.* **23**: 54–59.
38. Moskot, M., K. Bochenska, J. Jakobkiewicz-Banecka, B. Banecki, and M. Gabig-Ciminska. 2018. Abnormal sphingolipid world in inflammation specific for lysosomal storage diseases and skin disorders. *Int. J. Mol. Sci.* **19**: E247.
39. Sawai, H., and Y. A. Hannun. 1999. Ceramide and sphingomyelinases in the regulation of stress responses. *Chem. Phys. Lipids.* **102**: 141–147.
40. Fartasch, M., M. L. Williams, and P. M. Elias. 1999. Altered lamellar body secretion and stratum corneum membrane structure in Netherton syndrome: differentiation from other infantile erythrodermas and pathogenic implications. *Arch. Dermatol.* **135**: 823–832.
41. Bonnard, C., C. Deraison, M. Lacroix, Y. Uchida, C. Besson, A. Robin, A. Briot, M. Gonthier, L. Lamant, P. Dubus, et al. 2010. Elastase 2 is expressed in human and mouse epidermis and impairs skin barrier function in Netherton syndrome through filaggrin and lipid misprocessing. *J. Clin. Invest.* **120**: 871–882.
42. Hachem, J. P., F. Wagberg, M. Schmuth, D. Crumrine, W. Lissens, A. Jayakumar, E. Houben, T. M. Mauro, G. Leonardsson, M. Brattsand,

- et al. 2006. Serine protease activity and residual LEKTI expression determine phenotype in Netherton syndrome. *J. Invest. Dermatol.* **126**: 1609–1621.
43. Hachem, J. P., D. Crumrine, J. Fluhr, B. E. Brown, K. R. Feingold, and P. M. Elias. 2003. pH directly regulates epidermal permeability barrier homeostasis, and stratum corneum integrity/cohesion. *J. Invest. Dermatol.* **121**: 345–353.
44. Lee, S. E., S. K. Jeong, and S. H. Lee. 2010. Protease and protease-activated receptor-2 signaling in the pathogenesis of atopic dermatitis. *Yonsei Med. J.* **51**: 808–822.
45. Furio, L., and A. Hovnanian. 2014. Netherton syndrome: defective kallikrein inhibition in the skin leads to skin inflammation and allergy. *Biol. Chem.* **395**: 945–958.
46. Uche, L. E., G. S. Gooris, C. M. Beddoes, and J. A. Bouwstra. 2019. New insight into phase behavior and permeability of skin lipid models based on sphingosine and phytosphingosine ceramides. *Biochim. Biophys. Acta Biomembr.* **1861**: 1317–1328.
47. Leung, A. K. C., B. Barankin, and K. F. Leong. 2018. An 8-Year-Old Child with Delayed Diagnosis of Netherton Syndrome. *Case Rep. Pediatr.* **2018**: 9434916.